Chapter 10
Electronic traps in organic transport layers

R. Schmechel and H. von Seggern, phys. stat. sol. (a) **201**, 1215 (2004)

2009. 5. 7.

Changhee Lee
School of Electrical Engineering and Computer Science
Seoul National Univ.
chlee7@snu.ac.kr

Disorder

• Potential Wells for Crystalline Lattice

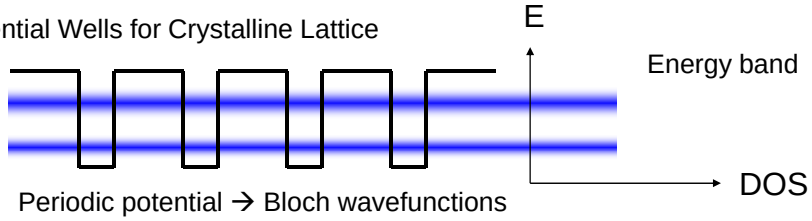

Periodic potential → Bloch wavefunctions

• Sufficient disorder produces localized states (P. W. Anderson)

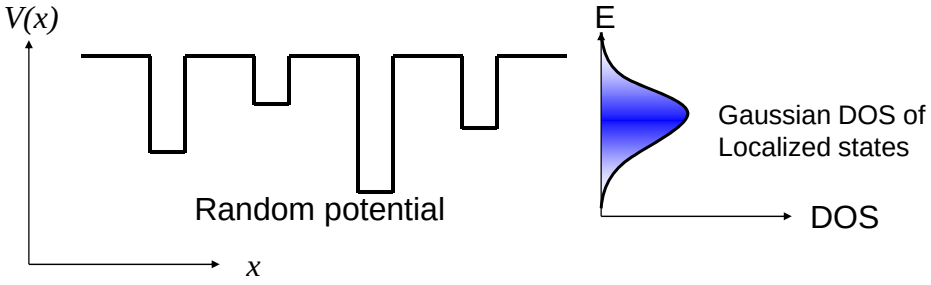

Narrow band width and hopping transport

• **Weak van der Waals interaction between molecules**

→ Each molecule keep its molecular levels independent of surrounding matrix in solid

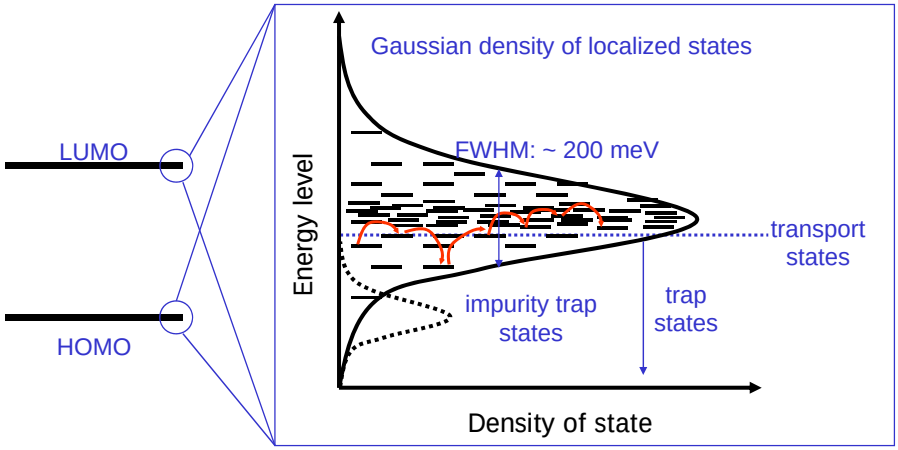

Traps: Localized states below transport states

Origin of traps states

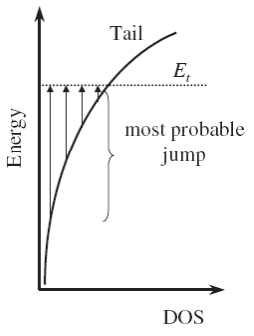

Fig. 2 Most probable jump of a carrier from a tail state to the transport energy E_t.

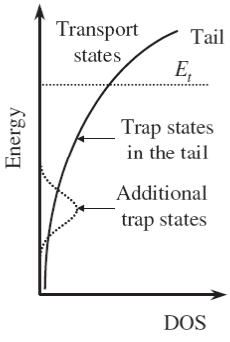

Fig. 3 Trap states in the tail, additional trap states and regular transport states.

1. *Impurities*
2. *Structural Defects*
3. *Geminate pairs → Coulomb trap.*
4. *Self-trapping*

R. Schmechel and H. von Seggern, phys. stat. sol. (a) **201**, 1215 (2004)

Trap detection techniques

1. The trap states are first filled, usually at low temperatures, to prevent a fast escape.
- **photogeneration** of charge carriers: produces simultaneously both types of charge carriers
- **electrical injection**

2. The trapped charge carriers are released in a controlled way.
- ***optically stimulated current* (OSC):** trapped charge carriers are detrapped by interaction with light and the resulting current is recorded as a function of the wavelength of the light. But there is a restriction due to optical selection rules.
- ***thermally stimulated currents* (TSC):** the trapped charge carriers are released by heating up the sample with a linear temperature ramp, while the stimulated current is recorded as function of temperature. This directly yields the required activation energies for the charge transport independent of any selection rules.
- ***thermally stimulated luminescence* (TSL):** To overcome the problem of the unknown temperature dependence of the mobility, the luminescence due to radiative recombination is recorded. Such luminescence is most probably related to recombination of geminate pairs.

** TSL and TSC are therefore complementary techniques. Each carrier, which recombines and produces a TSL signal, will lower the TSC signal and vice versa each not recombining carrier enhances the TSC signal. Thus, if possible, TSL and TSC should be recorded simultaneously.*

- ***photo-induced absorption* (PIA):**
- ***electroabsorption:*** knowledge about the internal field strength produced by trapped charge carriers
- ***time-of-flight (TOF) techniques and I–V characteristics in the space charge limited current (SCLC) regime:*** information on the charge carrier mobility
- ***impedance spectroscopy:*** information on trap depth and trap energy distributions.

R. Schmechel and H. von Seggern, phys. stat. sol. (a) **201**, 1215 (2004)

TOF-PC Mobility – Effect of traps

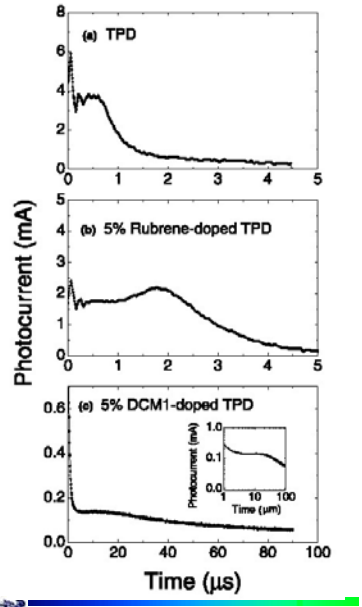

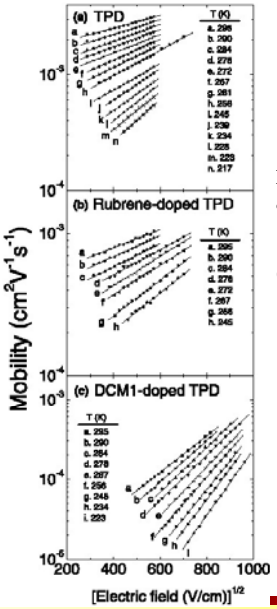

Doping reduces carrier mobility and affects I-V-EL characteristics.

Ref. H.H. Fong et al.
Chem. Phys. Lett. 353 (2002) 407

Influence of traps on the carrier mobility

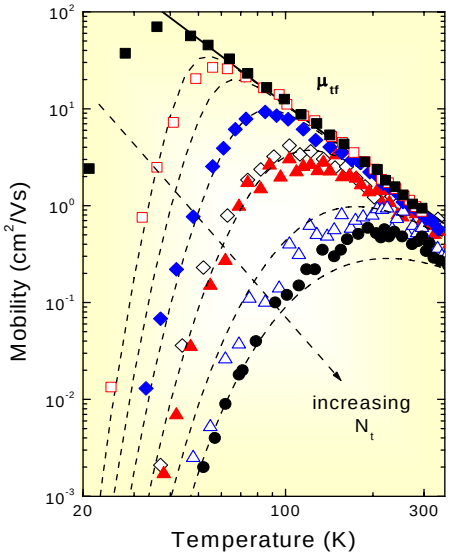

Exponential Decrease of μ
E_t ~ 40 - 50 meV

Dependence on Trap Density N_t
N_t ~ 10^{16} - 10^{18} cm^{-3}

Trap-Free Limit : Power Law T^{-n}
n ~ 1.6 - 2.3
phonon scattering

J. H. Schön et al.
Phys. Rev. B **63**, 245201 (2001)

TSC/TSL

If an energy distribution of the trap states exists, TSC and TSL spectra are a complicated convolution of contributions from different traps at different energies. To demerge the information, fractional techniques have to be applied.

- The shallowest occupied traps mainly determine the initial rise of a TSC/TSL signal.
- If a previously fractional heating process up to a specific temperature T_{stop} already has emptied the shallowest traps, the next deeper lying occupied traps determine the initial rise (Fig. 4a).
- The whole trap spectrum can be scanned by a stepwise increase of the pre-heating temperature T_{stop}. (Fig. 4b). The area between different main runs is a measure for the released charge in the respective T_{stop} interval.
- Each released charge per T_{stop} interval can be related to the activation energy obtained from the initial rise. This yields an image of the density of occupied states.

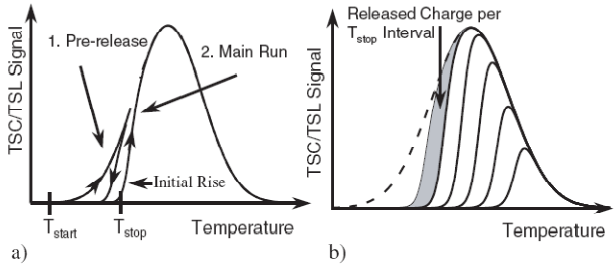

Fig. 4 Basic principle of fractional TSC/ TSL technique: (a) Basic cycle consisting of pre-release and main run, (b) different main runs for different T_{stop} temperatures of the pre-run; spectra are only schematically.

R. Schmechel and H. von Seggern, phys. stat. sol. (a) **201**, 1215 (2004)

Typical TSC results of single layer devices

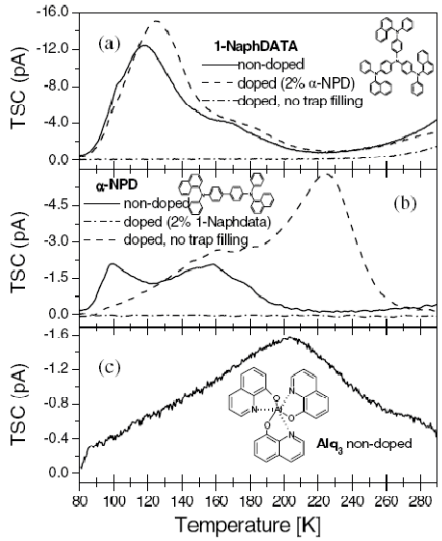

R. Schmechel and H. von Seggern, phys. stat. sol. (a) **201**, 1215 (2004)

Organic Semiconductor
EE 4541.617A
2009. 1st Semester

Typical TSC results of single layer devices

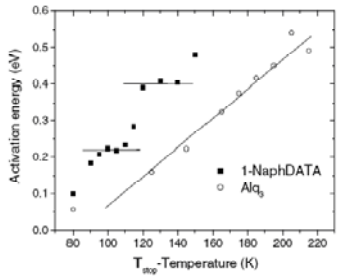

Fig. 6 Comparison of experimentally derived activation energies for 1-NaphDATA and Alq_3 as a function of T_{stop} temperature derived from the T_{start}–T_{stop} method.

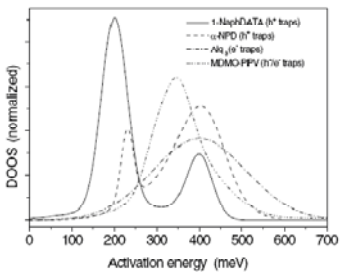

Fig. 7 Density of occupied states (DOOS) as determined by a fractional TSC method for the most prominent small molecule transport materials as indicated. All curves were obtained from optical trap filling at 80 K under a small bias of –0.3 V. The curves are normalized to an equal number of charges.

The nature of such isolated TSC peaks is related either to impurity defects or structural defects.
- hole transport materials (α-NPD or 1-NaphDATA) show a more discrete trap spectrum
- Alq3 reveals a broad distribution of trap states.

* An essential difference between the HTMs and Alq3 is the anisotropic molecular structure of the HTMs compared to a more globular appearance of Alq3.

→ HTMs: preferred orientations during layer growth allowing specific orbital overlap to dominate.
→ Alq3: globular shape allows a variety of energetically and structurally different neighborhoods

R. Schmechel and H. von Seggern, phys. stat. sol. (a) **201**, 1215 (2004)

TSC spectra of Alq3 batches from different suppliers

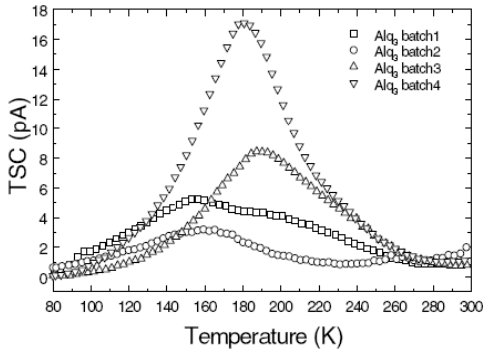

Fig. 8 TSC spectra of Alq_3 batches from different industrial suppliers obtained for identical deposition and TSC conditions. These results were obtained within confidential industrial cooperations and therefore the suppliers are not mentioned explicitly.

Different batches of Alq3 from different suppliers yield different TSC peaks.
→ presence of specific impurities or different Alq3 conformations?

R. Schmechel and H. von Seggern, phys. stat. sol. (a) **201**, 1215 (2004)

TSC spectra of Alq3 devices

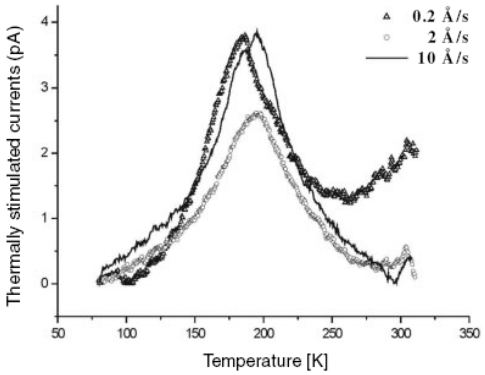

Fig. 18 TSC spectra of ITO/Alq_3/Al samples fabricated utilizing different evaporation rates of 0.2 Å/s, 2 Å/s and 10 Å/s. Trap filling was performed optically at 80 K at a wavelength of 400 nm.

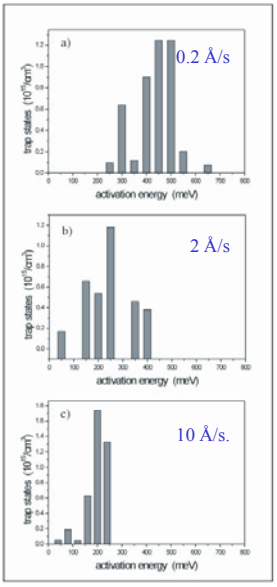

R. Schmechel and H. von Seggern, phys. stat. sol. (a) **201**, 1215 (2004)

TSC spectra of α-NPD devices

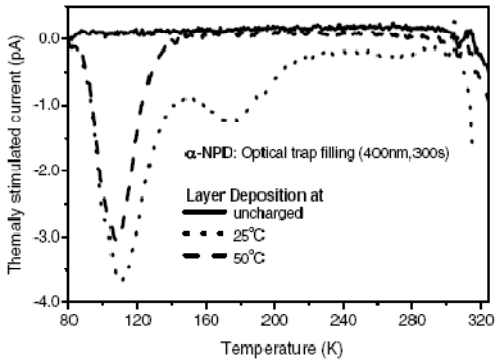

Fig. 20 TSC spectra of α-NPD single layer devices, the substrate of one sample was heated during evaporation as indicated. Traps were filled by optical exposure under a small electrical bias of −0.3V.

R. Schmechel and H. von Seggern, phys. stat. sol. (a) **201**, 1215 (2004)

Effect of doping on electronic traps: α-NPD doped with 1-NaphDATA

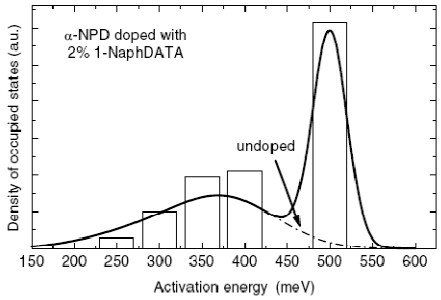

Fig. 9 Density of occupied states of an α-NPD layer doped with 2% of 1-NaphDATA. The traps were optically filled at 80 K for 5 min. The bars present the released charge at specific activation energies (measured as described in chapter 3), the line is a guideline for the eye.

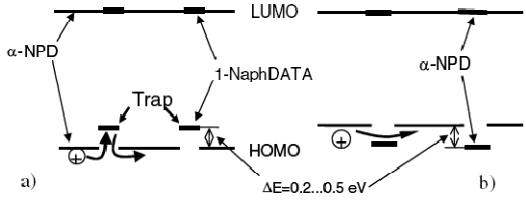

Fig. 10 Energy level scheme of (a) 1-NaphDATA in α-NPD acting as a trap state and (b) α-NPD in 1-NaphDATA acting as a scattering center.

R. Schmechel and H. von Seggern, phys. stat. sol. (a) **201**, 1215 (2004)

Effect of doping on electronic traps: Alq3 doped with rubrene

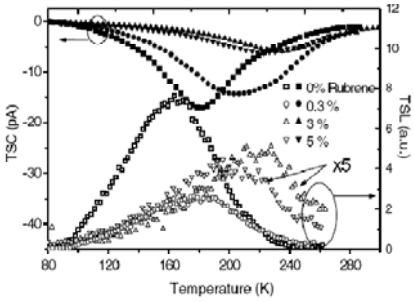

Fig. 11 Effect of Rubrene doping on the TSC and TSL spectra of Alq_3. The Rubrene concentration was varied between 0 and 5%.

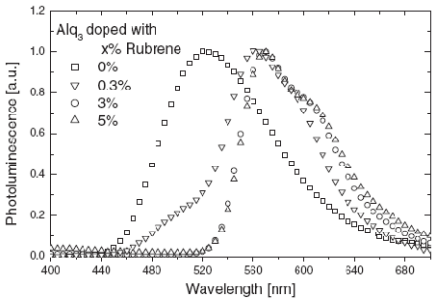

Fig. 12 Photoluminescence spectra of Rubrene doped Alq_3 for different Rubrene concentrations as indicated.

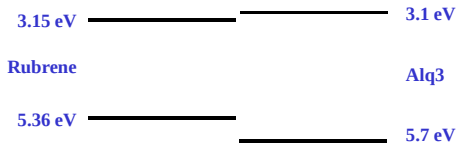

R. Schmechel and H. von Seggern, phys. stat. sol. (a) **201**, 1215 (2004)

α-NPD doped with 1-NaphDATA

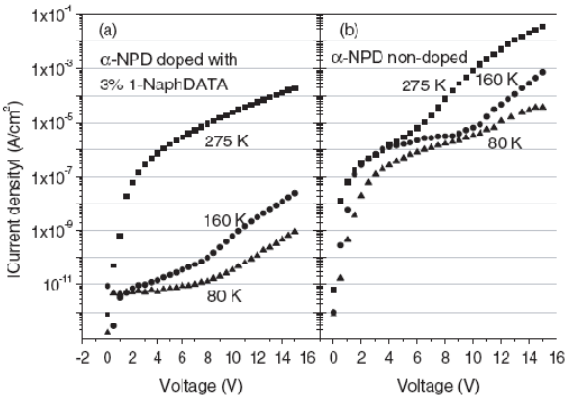

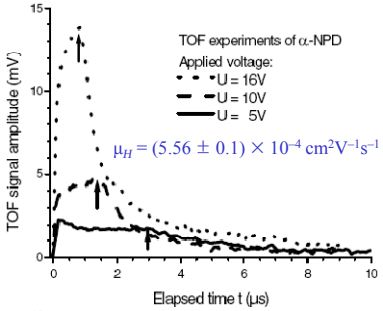

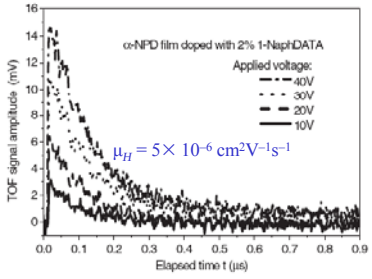

R. Schmechel and H. von Seggern, phys. stat. sol. (a) **201**, 1215 (2004)

I-V dependence of OLEDs with doped HTLs

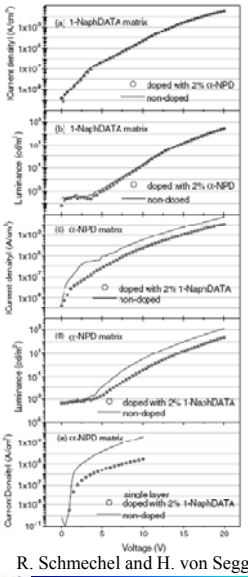

Fig. 16 *I–V* and *L–V* characteristics of an OLED (ITO/HTL/Alq_3/Al) utilizing doped (circles) and non-doped (lines) α-NPD and 1-NaphDATA (a–d) and an α-NPD single layer device (e) measured in ambient air at room temperature.

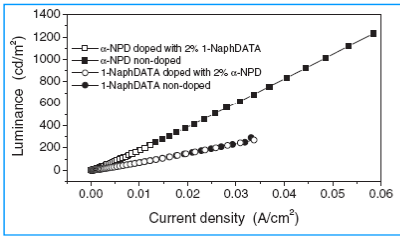

Fig. 17 Luminance vs. current density for 1-NaphDATA doped in α-NPD and α-NPD doped in 1-NaphDATA.

R. Schmechel and H. von Seggern, phys. stat. sol. (a) **201**, 1215 (2004)

TSC spectra of polymers

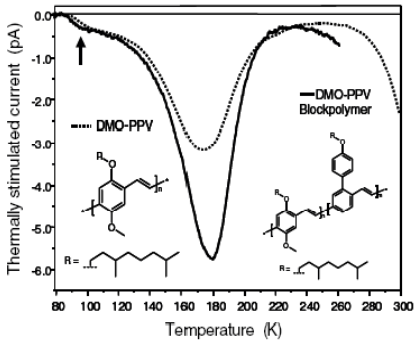

Fig. 21 Conventional TSC spectra of the investigated polymers DMO-PPV and DMO-PPV (BP) in an ITO/polymer/Al device.

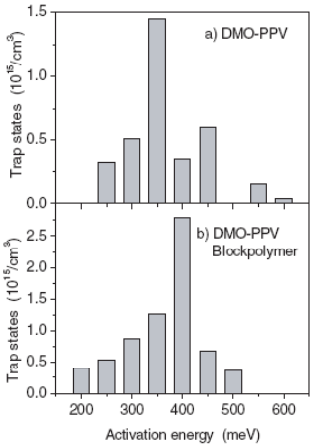

Fig. 22 Density of occupied states of DMO-PPV (a) and the DMO-PPV blockpolymer (b).

R. Schmechel and H. von Seggern, phys. stat. sol. (a) **201**, 1215 (2004)

TSC spectra of DMO-PPV

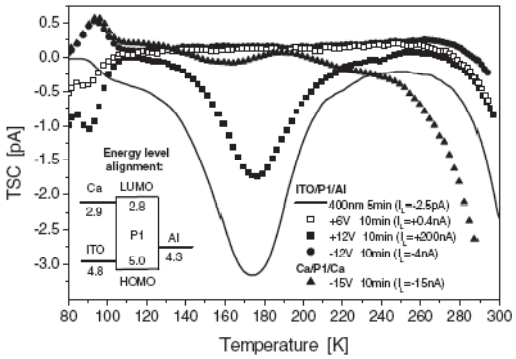

Fig. 23 TSC spectra of electrical and optical trap filled DMO-PPV. The trap-filling conditions are indicated in the figure. TSC is always performed under a bias voltage of –0.3 V.

R. Schmechel and H. von Seggern, phys. stat. sol. (a) **201**, 1215 (2004)